Removal of monoethylene glycol from wastewater by using Zr-metal organic frameworks

Sami Zaboon[a], Hussein Rasool Abid[a,b*], Zhengxin Yao[a] , Rolf Gubner[a], Shaobin Wang[a], Ahmed Barifcani[a]

[a] Department of Chemical Engineering, Curtin University, GPO Box U1987, Perth, WA, 6845, Australia.

[b] Environmental Health Department, Faculty of Applied Medical Science, University of Kerbala, Karbala, Iraq

*Corresponding author: Tel. +61892665411,

E-mail address: Hussein.Abid@curtin.edu.au, hr_aust2009@yahoo.com.au

Abstract

Mono-ethylene glycol (MEG), used in the oil and gas industries as a gas hydrate inhibitor, is a hazardous chemical present in wastewater from those processes. Metal-organic frameworks (MOFs) (modified UiO-66* and UiO-66-2OH) were used for the effective removal of MEG waste from effluents of distillation columns (MEG recovery units). Batch contact adsorption method was used to study the adsorption behavior toward these types of MOFs. Adsorption experiments showed that these MOFs had very high affinity toward MEG. Significant adsorption capacity was demonstrated on UiO-66-2OH and modified UiO-66 at 1000 mg. g^{-1} and 800 mg. g^{-1} respectively. The adsorption kinetics were fitted to a pseudo first-order model. UiO-66-2OH showed a higher adsorption capacity due to the presence of hydroxyl groups in its structure. A Langmuir model gave the best fitting for isotherm of experimental data at pH = 7.

Keywords: Mono-Ethylene Glycol, UiO-66, UiO-2OH, wastewater, adsorption kinetic, isotherms

* Material was synthesized by University of Oslo

Introduction

Natural resources have become a hot topic in current scientific research, in an effort to maintain and preserve the Earth's environment for continued human life [1, 2]. In this regard, petroleum pollution is a major global problem [3]. Mono-ethylene glycol (MEG) is a petroleum pollutant, which is a colorless, odorless, and slightly viscous liquid, more hygroscopic than glycerol and miscible with water in all proportions. [4, 5]. The US Environmental Protection Agency has established a standard of less than 7 mg L^{-1} of MEG in drinking water [6, 7]. MEG can cause damage to the kidneys or death at high accumulated concentrations [8]. Natural gas processing produces ethylene glycol-containing wastewater and consequently increases the chemical oxygen demand (COD) in water [9]. Removal of MEG from contaminated water is thus an important consideration in the design of operation units in the petroleum industry [10].

There are three principal treatment processes for removal of MEG from wastewater: filtration [11], biological [12] and adsorption processes [9]. Moreover, nanofiltration and membrane technologies are widely used to separate low molecular organic pollutants (such as MEG) from water [11], but these methods have several challenges such as membrane fouling, chemical resistance and limited lifetime of membranes, insufficient separation, generation of a concentrate and Insufficient rejection for individual compounds [13]. Microorganisms are also used for the removal of MEG, diethylene glycol (DEG), and triethylene glycol (TEG) [14], but biological treatment is incapable of the elimination of the pollutants in a continuous process [15].

Adsorption is a more reliable and economically feasible method in this regard, and has already been used in advanced water treatment [16, 17]. Activated carbon [9, 18, 19] and zeolite [20, 21] are common porous materials used for physical sorption. Recently, metal organic frameworks (MOFs) have been intensively studied for use in water treatment. Many MOFs, such as Zr-MOF (UiO-66) [22], ZIF-67 [23-25], HKUST-1 [26, 27], MIL-101, and MIL-100 [28, 29] have been successfully tested for adsorption of specific contaminants in water. In this unprecedented work, we use modified UiO-66 and UiO-66-2OH with a high pore volume, nano-crystal size and high water stability to effectively capture MEG from wastewater in the case of distillation failure. This batch adsorption process was conducted at different contact time and pH values.

Experimental adsorption capacities were obtained for different concentrations in effluent wastewater, and adsorption kinetics and isotherms were studied.

Materials and Methods

All chemicals including *N,N*-dimethylformamide (DMF, 99%), 1,4-benzenedicarboxylic acid (BDC, 98.9%), ammonium hydroxide (NH_4OH, 24%), 2,5-dihydroxyterephthalic acid (DHBDC, 98%), zirconium chloride ($ZrCl_4$, ≥99.5%), absolute methanol (CH_3OH, ≥ 99.9%), absolute ethanol (C_2H_6O, ≥99.8) and acetic acid (CH_3COOH, ≥99.7%) were purchased from Sigma Aldrich and used without further purification. Deionized water was supplied from an ultra-high pure water system in the laboratory.

Synthesis

UiO-66-2OH was synthesized solvothermally according to a previously reported co-solvent procedure [30]. $ZrCl_4$ (5.150 mmol) and DHBDC (2.63 mmol) were dissolved in DMF (774.93 mmol, 60 mL). After 15 min of mixing, acetic acid (174.68 mmol) and absolute ethanol (171.26 mmol) were added to the mixture. The solution was then transferred in a 125 mL Parr PTFE-lined stainless steel vessel (Parr Instrument Company, USA), which was sealed and heated in a preheating oven at 676 K for 48 h. Greenish-yellow crystals were then extracted as a product by vacuum filtration.

For activation of UiO-66-2OH, a solvent exchange method by methanol was used by mixing 100 mg of sample material in 50 mL of absolute methanol for approximately 15 min, and then soaked for 3 d. After that, the product was separated by vacuum filtration and heated at 373 K for 2 h and further heated under vacuum at 453 K for 2 d.

Modified UiO-66 was synthesized solvothermally according to a reported procedure by a single-solvent method [31]. A solution of 405.38 mmol DMF was divided equally into two batches. In the first batch, 2.27 mmol BDC was added and mixed for 15 min and then NH_4OH (0.4 mL, 2 M) was added dropwise to this mixture. In the second batch, 2.27 mmol of $ZrCl_4$ was mixed with the solvent for approximately 30 min. After that, both batch solutions were mixed for approximately 20 min. Finally, the resulting solution was placed inside a 45 mL Parr PTFE-lined stainless steel vessel (Parr Instrument Company, USA) and placed in an oven at 393 K for 24 h. After cooling to room temperature, vacuum filtration was used to separate white gel-like materials,

which were dried in an oven at 353 K for 24 h. For activation of modified UiO-66, a solvent exchange method by chloroform was used by mixing 100 mg of sample material in 50 mL of chloroform for 30 min, and then soaked for 5 d. Then, the product was filtered by vacuum filtration and dried in the oven at 373 K for 2 h. The final product was heated under vacuum at 473 K for 2 d.

Characterization

Powder X-ray diffraction (XRD) patterns were obtained by using an XRD diffractometer with CuKα radiation (λ=1.5406 Å) at 2θ=5–70° to identify the structure of the synthesized material and its structural integrity. Morphological characterization was performed by scanning electron microscopy (SEM; Zeiss Neon 40 EsB FIB/SEM beam). FTIR spectra were obtained using a SpectrumTM 100 FT-IR (PerkinElmer) to investigate the functional groups in UiO-66 over a scan range of 650–4500 cm^{-1}. A Quantachrome instrument (Autosorb-1) was used to determine N_2 adsorption/desorption isotherms for pore analysis including pore volume and surface area. A quartz thimble was filled by a 20 mg of sample and then it was preheated in an oven at 393 K for at least 2 h. After that, the sample was degassed at 453 K for 2 d and then transferred to an analysis port for analysis. Thermal stability of MOFs was determined by thermogravimetric analysis (TGA; TGA/DSC1 STARe system-METTLER TOLEDO). In a typical analysis, 10 mg of sample was loaded into an alumina pan in the TGA furnace and heated under 20 $mL \cdot min^{-1}$ air flow at a ramping rate of 10 K/min from room temperature to 1173 K. Zeta potential was determined by a Zetasizer Nano-ZS (Malvern Instruments) at 298 K.

Adsorption Studies

Adsorption studies of MEG from wastewater using modified UiO-66 and UiO-66-2OH were conducted using the batch contact adsorption method. Briefly, six samples of MEG were prepared at different concentrations (700, 600, 500, 400, 300, and 150 $mg \cdot L^{-1}$). Then 20 mg of the adsorbents was placed in 40 mL of the MEG solution, which was agitated by a magnetic stirrer for different periods at pH = 7 and 3. A PVDF-0.45 micron syringe filter was used to separate the adsorbents from the aqueous solution and the supernatant solution was measured using an ATAGO refractometer (ATAGO) PAL-Cleaner- 4536.

The adsorbed amount of MEG (q_t) and the removal efficiency (R%) were calculated by Eqs. (1) and (2), respectively.

$$q_t = \frac{(C_o - C_t).V}{m} \quad (1)$$

$$R\% = \frac{(C_o - C_t).100}{C_o} \quad (2)$$

The batch adsorption was also carried out at pH = 3, 5, 8 and 10 for a fixed contact time of 24 h.

Regeneration of the adsorbent was carried out by washing the loaded adsorbents with ultra-high pure water at 373 K for several cycles.

Recycling tests of adsorbents

Modified UiO-66 and UiO-66-2OH were separately suspended in MEG solutions in a ratio of 1:2 using MEG concentration of 600 mg L^{-1} at pH 7 for mixing around 60 min. Then UiO-66 materials were filtered by syringe filter (0.45 µm, PVDF) and supernatant was tested for remaining concentration of MEG to calculate the removal efficiency. The net collected weight was washed by hot water (373 K) three times. Next, the sample was dried in the oven at 393 K for 2 h. The dried adsorbent was used for next cycle of MEG removal. The same procedure was repeated for 5 cycles with carefully adjusting an amount of the solution with a net weight of adsorbents at the same conditions.

Results and Discussion

Characterization

Figure 1 depicts XRD patterns of UiO-66-2OH and modified UiO-66 after activation, which were exactly similar to those of original UiO-66 as shown in previous literature [32]. These MOFs demonstrate robust behavior over a wide pH range (3–10) as shown in Figure S1 and Figure S2. However, the modified UiO-66 displayed higher water stability than UiO-66-2OH as noted by the absence of some small peaks at high 2θ values on the pattern of UiO-66-2OH after exposure to MEG solution at pH = 10.

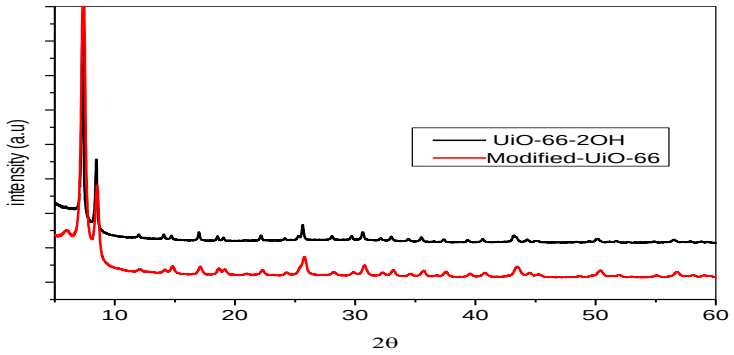

FIG.1 XRD patterns of UiO-66-2OH and modified-UiO-66 after activation.

The spectra in Figure 2 demonstrate the functional groups on modified UiO-66 and UiO-66-2OH. The carboxyl groups (COOH) of BDC and DMF molecules at 1659 cm^{-1} [32] were completely disappeared after activation. In addition, in the spectrum of UiO-66-2OH, two peaks are present for hydroxyl groups at 1460 cm^{-1} and the broad peak at 3000–3680 cm^{-1}. Coordinated carboxyl groups of benzene-1, 4,-dicarboxylates with zirconium nodes to form building block units of the structure $(Zr_6O_4)(OH)_4(CO_2)_n$ were present at 1500 and 1380 cm^{-1} [33] in modified UIO-66 and UiO-66-2OH. Figure S3 shows the spectra of UiO-66-2OH at pH = 3, 7 and 10 as compared with the spectrum of UiO-66-2OH before adsorption use. The structure of UiO-66-2OH was clearly present based on the decreased peak intensities at 1500 and 1380 cm^{-1}. On the other hand, new peaks emerged at 1740–1750 cm^{-1}, which are related to carbonyl carbons of UiO-66-2OH conjugated with MEG. Likewise, the peak of hydroxyl groups at 3000–3680 cm^{-1} was more intense, indicating a high amount of loaded MEG in the pores. Figure S4 shows spectra of modified UiO-66 used for MEG adsorption at different pH values. All the spectra describe the integrity of the structure, as all peaks in modified UiO-66 prior to MEG adsorption are observed on the spectra of modified UiO-66 after use at pH = 3, 7 and 10. The intensity of hydroxyl groups on the spectrum of used modified UiO-66 was significantly increased due to the high load of MEG inside the pores. In addition, there is a trace of MEG conjugated with carbonyl carbons of modified UiO-66 after use at pH = 7 and 10, shown by the peak at 1740 cm^{-1}.

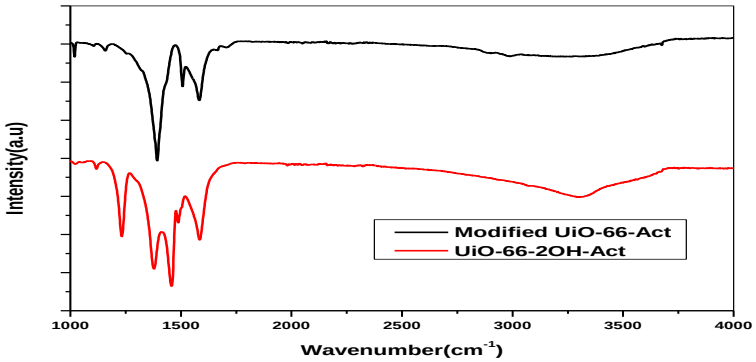

FIG.2 FTIR spectra of modified-UiO-66 and UiO-66-2OH after activation.

N_2 adsorption and desorption isotherms of UiO-66-2OH are shown in Figure 3(a), which is of H4 type (IUPAC classification) [34] with a hysteresis loop at a wide range of relative pressure. It was observed, the hysteresis loop is accompanied by capillary condensation in neck bottle pores [35]. UiO-66-2OH is a mostly mesoporous material with several peaks (3.1, 4.8, 7.6, and 12.5 nm) as shown in Figure 3(b). In addition, the micropore distribution was determined with the peak at 2 nm (Figure 3(c)). The pore volume is approximately 0.63 $cm^3 \cdot g^{-1}$ and the BET surface area is 473 $m^2.g^{-1}$, smaller than those of UiO-66 [36, 37] but slightly higher than those of UiO-66-2OH in a previous study [30]. The external surface area is 289 $m^2.g^{-1}$. Figure 4(a) shows N_2 adsorption/desorption isotherms of modified-UiO-66, displaying a narrow hysteresis loop in a wide range of relative pressure. Figure 4(b) shows three mesopore peaks (3.7, 6.7 and 15.4 nm) while Figure 4(c) illustrates the micropore distribution in single peak at 1.4 nm. The BET surface area and pore volume are 1273 $m^2.g^{-1}$ and 1.63 $cm^3.g^{-1}$, respectively, whereas the external surface area is 331 $m^2.g^{-1}$.

The BET surface areas of UiO-66-2OH and modified UiO-66 after adsorption of MEG were reduced, giving 255 and 704 $m^2.g^{-1}$, respectively. The reduction in surface area may attribute to porosity loss [36] as a result of adsorption of MEG and it may also be related to the defect of the structure[37, 38]. Figure S5 (a) shows N_2 adsorption/desorption isotherm on modified UiO-66 with sharp increasing in relative pressure close to the unity while the hysteresis loop was limited in very narrow range at relative pressure of 0.85, indicating that pore connectivity is high. Figure S5 (b) demonstrates a single peak mesopore distribution at 30 nm, which is larger than the mesopore size before the adsorption. The larger mesopore was due to high cavity

created during water diffusion. Figure S5(c) displays the micropore diameter of 0.6 nm because of blocking of smaller pores by adsorbate molecules[39].

Figure S6 (a) shows N_2 adsorption/desorption isotherm on UiO-66-2OH. It is similar to that of modified UiO-66, which indicates the majority of meosopore. The mesopore and micropore distributions were represented in single peak at 4 and 0.64 nm as shown in Figure S6 (b) and (c), respectively. They are smaller than the pore sizes of the adsorbent before the adsorption process, suggesting that the most porous structure was occupied by MEG molecules.

The SEM images in Figure S7 (a) and (b) show the crystal morphology and crystal size of UiO-66-2OH and modified UiO-66, indicating a cubic geometry as the same as the original UiO-66. However, the primary particle size differed significantly. Modified UiO-66 featured nanoscaled crystals < 50 nm in size, while UiO-66-2OH crystals were approximately 100 nm in size. The reduction in crystal size of modified UiO-66 is caused by ammonium hydroxide additives [31], which enhance the solubility of the reactants used during synthesis [40]. Thermal stability of modified UiO-66 and UiO-66-2OH are shown in Figure S8, where the thermal stability of modified UiO-66 is higher than that of UiO-66-2OH. The structures of modified UiO-66 and UiO-66-2OH were maintained at temperature up to 740 K and 500 K, respectively. The thermal stability of modified UiO-66 is similar to that of original UiO-66 without modification, as shown in previous literature [41].

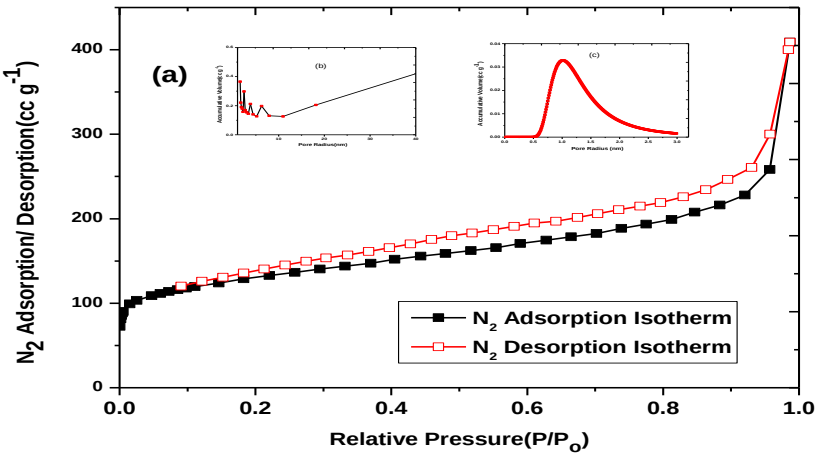

FIG.3 a) Adsorption/desorption isotherms of N_2 in UiO-66-2OH at 77 K, b) Mesopore distribution and c) Micropore distribution.

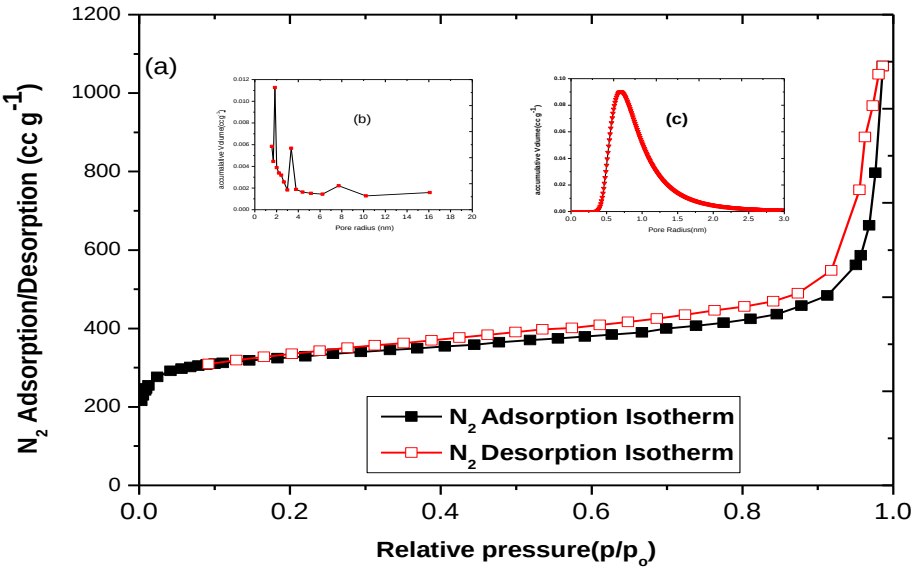

FIG.4 a) Adsorption/desorption isotherms of N_2 in modified-UiO-66 at 77K, b) Mesopore distribution and c) Micropore distribution.

Adsorption Studies

Effect of pH on adsorption

It is important to investigate the effect of acidity on the adsorption of MEG on the surface of modified UiO-66 and UiO-66-2OH. The distribution of acidic or basic molecules in pollutants is strongly dependent on acidity of the aqueous solution, and consequently their interaction with the surface of an adsorbent through adsorption processes [42]. When the solution is an acidic medium, the attractive force toward the surface of the adsorbent is enhanced. Hence, the adsorption capacity of MEG is increased as the pH decreases from 5 to 3, as shown in Figure 5. However, the presence of hydrogen ions in water and their attraction with molecules of MEG can affect the mobility of MEG via its movement toward the surface of adsorbents; this effect is noticed at pH < 5 on modified UiO-66. Neutral solutions (pH = 7) seems to be the best medium for adsorption of MEG. Specifically, UiO-66-2OH can interact via hydrogen bonds between the hydroxyl groups of UiO-66-OH and the hydroxyl groups of MEG. Meanwhile, the interaction between modified UiO-66 and MEG is likely to arise from electrostatic forces. In basic solutions, the adsorption of MEG is decreased,

when pH increases from 7 to 8 and 8 to10 in UiO-66-2OH and modified UiO-66 respectively, but in UiO-66-2OH, this influence is minimal at pH > 8.

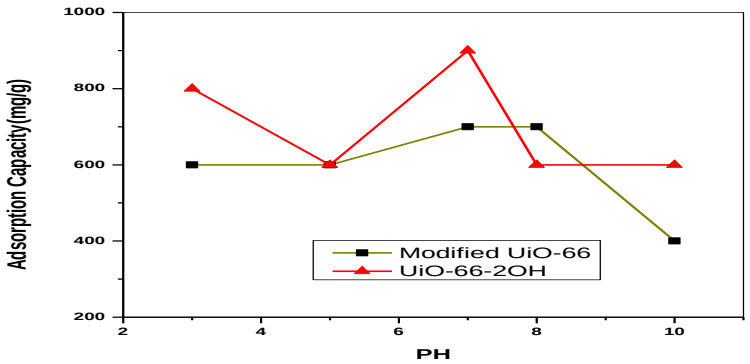

FIG.5 Effect of pH on the adsorption capacity of MEG on modified UiO-66 and UiO-66-2OH.

Kinetic Models

Active water treatment significantly depends on the adsorption kinetics, providing sufficient knowledge on the mechanism of adsorption. In this study, three popular models were investigated and fitted with experimental data. All parameters of the kinetic models are shown in Tables 1 and 2.

A pseudo-first order kinetic model (Lagergren) has been suggested for the adsorption of liquid/solid systems, depending on the adsorption capacity of the solid. The general linear form of the pseudo-first order equation [43] is expressed as:

$$\ln(q_e - q_t) = \ln(q_e) - k_f t \qquad (1)$$

where q_e and q_t are the adsorbed amounts of MEG (mg·g^{-1}) on modified UiO-66 or UiO-66-2OH at equilibrium or at time t (min), respectively, and k_f is the rate constant of the first order model (min^{-1}).

A pseudo-second order kinetic equation was determined by Ho and Mckay depending on the amount of adsorbate adsorbed on the adsorbent [44]. It can be expressed as:

$$\frac{t}{q_t} = \frac{1}{k_s {q_e}^2} + \frac{t}{q_e} \qquad (2)$$

where k_s is the second-order rate constant (g·mg^{-1}·min^{-1}).

The intra-particle diffusion equation [45] is important for interpreting the adsorption mechanism of MEG on modified UiO-66 and UiO-66-2OH. The linear equation can be described as:

$$q_t = k_d t^{\frac{1}{2}} + C \quad (3)$$

where k_d is the intra-particle diffusion rate constant (mg·g^{-1}·min$^{0.5}$).

Tables 1 and 2 demonstrate the parameters of the pseudo-first order, pseudo-second order and intra-particle diffusion equations for adsorption of MEG on modified UiO-66 and UiO-66-2OH. The pseudo-first order kinetic model is used to describe the mechanism of adsorption in the case of physisorption and diffusion. More specifically, Tables 1 and 2 show that the rate constant k_f is relatively dependent on the initial concentration of MEG. The rate constant of MEG adsorption on modified UiO-66 and UiO-66-2OH was uniformly increased with increasing initial concentration of MEG at neutral acidity (pH = 7) [46]. Interestingly, the rate of diffusion via UiO-66-2OH is faster than that in modified UiO-66. Calculated adsorption capacity values obtained using the pseudo-first order kinetic model are approximately similar to experimental values.

For the adsorption of MEG on modified UiO-66 and UiO-66-2OH, the correlation coefficients (R^2) at pH = 7 were 0.969 and 0.992, respectively, at an initial concentration of 700 ppm, while they were 0.913 and 0.938 at an initial concentration of 400 ppm. The fitting of experimental data at pH = 7 with the pseudo-first order kinetic model is given in Figure 6(a, b). In addition, R^2 values at pH = 3 were 0.985 and 0.991, respectively at 400 ppm, and 0.979 and 0.926 at 700 ppm; R^2 was increased by decreasing the initial concentration due to the impact of acidity at pH = 3. This can be observed in Figure 7(c, d), where the pseudo-first order kinetic model is in good agreement with the experimental data.

On the other hand, the pseudo-second order rate model was used to refer to chemisorption including valency forces through the sharing or exchange of electrons between adsorbates and adsorbent as covalent forces, and ion exchange [47]. As shown in Tables 1 and 2, the calculated values of adsorption capacity are fitted from experimental data. In addition, K_s values are mostly dependent on the initial concentrations of MEG in modified UiO-66 and UiO-66-2OH in acidic and basic conditions. Likewise, the R^2 values in the pseudo-second order model are lower than

R^2 observed in the pseudo-first order model, while they are slightly higher in modified UiO-66 than in UiO-66-2OH at pH = 3, where the average value of R^2 is 0.942 in modified UiO-66 and 0.891 in UiO-66-2OH. In contrast, R^2 values at pH = 7 are 0.931 and 0.957 for modified UiO-66 and UiO-66-2OH, respectively. The fitting of experimental data to a pseudo-second order rate model in modified UiO-66 and UiO-66-2OH is demonstrated in Figure 7(a, b) at pH = 7, and depicted in Figure 7 (c, d) for pH = 3. It seems that this model does not fit well with our experimental data. Based on this, adsorption of MEG on modified UiO-66 and UiO-66-2OH is likely preceded by diffusion and hydrogen bonding.

Table 1 Kinetic Parameters for MEG removal by modified UiO-66

Kinetic Model		Initial concentration of MEG in aqueous solution			
Pseudo-first order kinetic model					
pH	Parameter	700 ppm	600 ppm	500 ppm	400 ppm
7	K_f	0.018	0.017	0.014	0.0132
	q_e	818.5	737.4	623.6	523.1
	R^2	0.969	0.962	0.993	0.913
3	K_f	0.0174	0.015	0.0137	0.0151
	q_e	647.4	617.1	515.5	419.2
	R^2	0.979	0.942	0.931	0.985
Pseudo-second order kinetic model					
pH	Parameter	700 ppm	600 ppm	500 ppm	400 ppm
7	q_e	1000	909.1	769.2	769.2
	K_s	1.55×10^{-05}	1.40×10^{-05}	1.428×10^{-05}	8.24×10^{-06}
	R^2	0.969	0.959	0.953	0.845
3	q_e	833.33	833.3	769.2	555.6
	Ks	1.79×10^{-05}	1.15 x10E^{-05}	8.471×10^{-06}	1.80×10^{-05}
	R^2	0.969	0.934	0.929	0.935
Intraparticle diffusion					
pH	Parameter	700 ppm	600 ppm	500 ppm	400 ppm
7	K_d	88.5	79.7	61.3	62.1
	C	220.1	233.4	165.8	260.1
	R^2	0.986	0.992	0.964	0.962
3	K_d	87.3	70.9	60.1	46.9
	C	285.0	246.8	230.7	157.0
	R^2	0.978	0.986	0.963	0.994

Table 2 Kinetic Parameters for MEG removal by UiO-66-2OH

Kinetic Model	Initial concentration of MEG in aqueous solution				
Pseudo-first order kinetic model					
pH	Parameter	700 ppm	600 ppm	500 ppm	400 ppm
7	K_f	0.023	0.021	0.015	0.012
	q_e	980.3	879.3	796.9	704.6
	R^2	0.992	0.990	0.989	0.938
3	K_f	0.013	0.007	0.009	0.008
	q_e	896.9	824.1	716.9	617.7
	R^2	0.926	0.981	0.980	0.991
Pseudo-second order kinetic model					
pH	Parameter	700 ppm	600 ppm	500 ppm	400 ppm
7	q_e	1111	1000	1000	1111
	K_s	0.000027	3.28×10^{-05}	1.47×10^{-05}	5.59×10^{-06}
	R^2	0.984	0.985	0.981	0.880
3	q_e	1250	1250	1111	1000
	K_s	6.63×10^{-06}	5.18×10^{-06}	4.56×10^{-06}	4.34×10^{-06}
	R^2	0.90	0.950	0.817	0.90
Intraparticle diffusion					
pH	Parameter	700 ppm	600 ppm	500 ppm	400 ppm
7	K_{id}	127.2	82.9	76.1	80.2
	C	263.3	47.9	140.7	315.6
	R^2	0.935	0.997	0.966	0.967
3	K_{id}	109.0	76.1	67.3	54.5
	C	417.2	240.7	254.1	208.6
	R^2	0.99	0.966	0.923	0.990

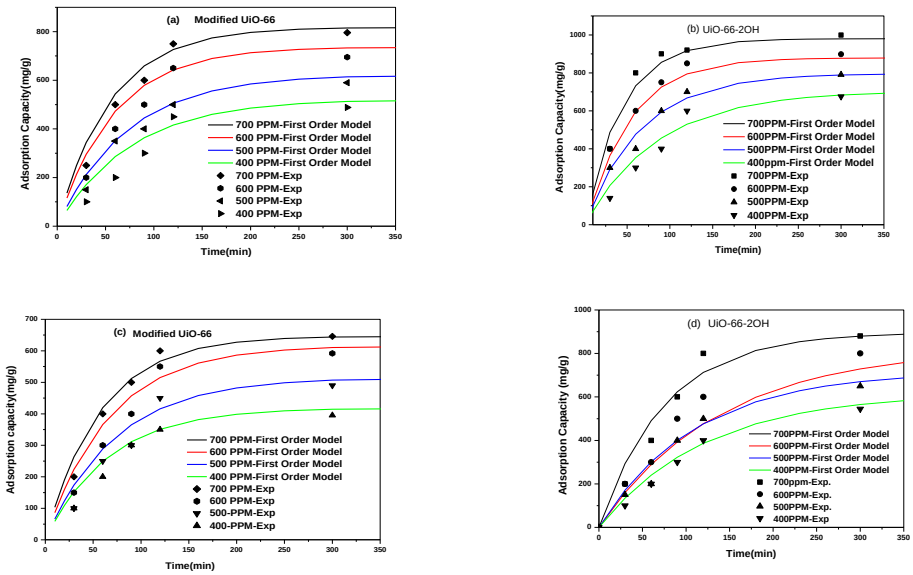

FIG.6 Comparison between the measured and pseudo-first order modelled time profiles for adsorption of MEG on modified UiO-66 and UiO-66-2OH at pH = 7 (a,b) and pH = 3 (c,d)

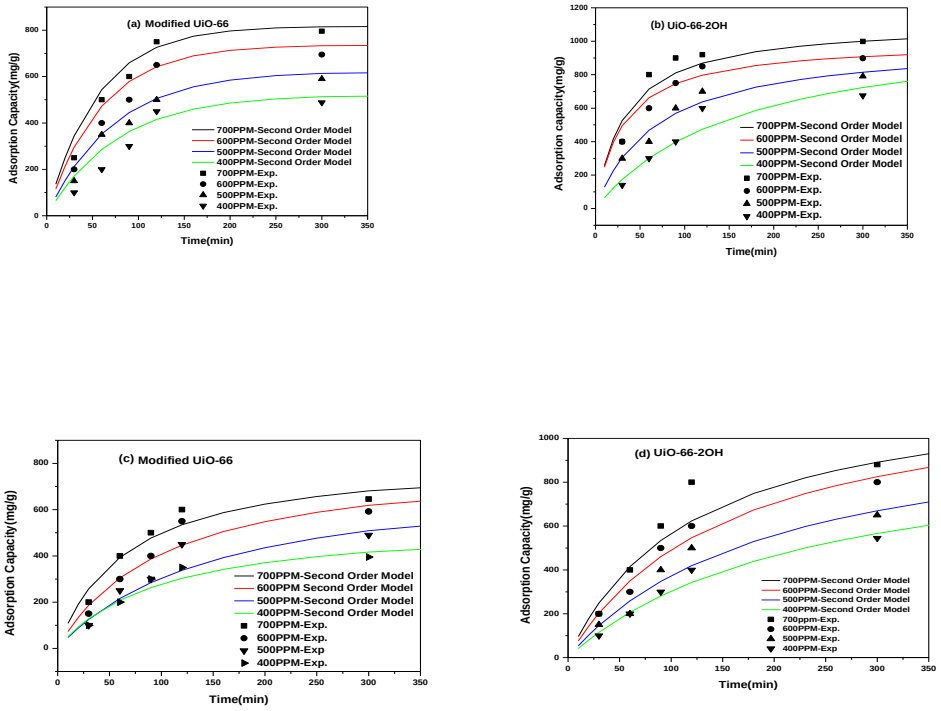

FIG.7 Comparison between the measured and pseudo-second order modelled time profiles for adsorption of MEG on modified UiO-66 and UiO-66-2OH at pH = 7 (a,b) and pH = 3 (c,d)

The effect of intra-particle diffusion resistance on the adsorption in this system was explored using equation (3) and the parameters are reported in Tables 1 and 2, which were obtained from the slope of the first step on the plot of adsorption capacity (mg/g) at any time against the square root of time ($min^{0.5}$), as shown in Figure 9 (a, b, c, d). Tables 1 and 2 show that the diffusion rate increases with increasing initial concentration due to the high driving force at high initial concentrations [48]. Moreover, UiO-66-2OH is faster than the modified UiO-66 because the diffusion rate is significantly dependent on the polarity of the pores, which is better in UiO-66-2OH due to the presence of hydroxyl groups. In addition, the diffusion rate during the migration of MEG molecules from bulk solution to the surface of the adsorbent [49] decreases somewhat in acidic solutions, which can be attributed to the increased number of protons (H^+) in solution and their attraction with MEG molecules. Three steps are shown in Figure 9; the first step is related to the high rate of diffusion for MEG molecules via water toward the adsorbents (besides the diffusion on the external surface of the adsorbents), the second step is the diffusion of MEG molecules inside

the pores of modified UiO-66 and UiO-66-2OH, and the third step is a move to equilibrium of the adsorption processes between MEG molecules and adsorbents. The second step in Figure 9(d) also shows that the rate of intra-diffusion inside the pores is higher than that in Figure 9(a, b, c). This can be justified according to the enhanced attractive forces for MEG molecules toward the surface of the adsorbent by increasing the concentration of H^+ with decreasing pH [49], and consequently the large pores are easily accessed by positive charges. This may enhance the positive charges of electrostatic interactions on the surface of the pores, and the hydrogen bonding interactions (from hydroxyl groups in UiO-66-2OH) may be significantly enhanced.

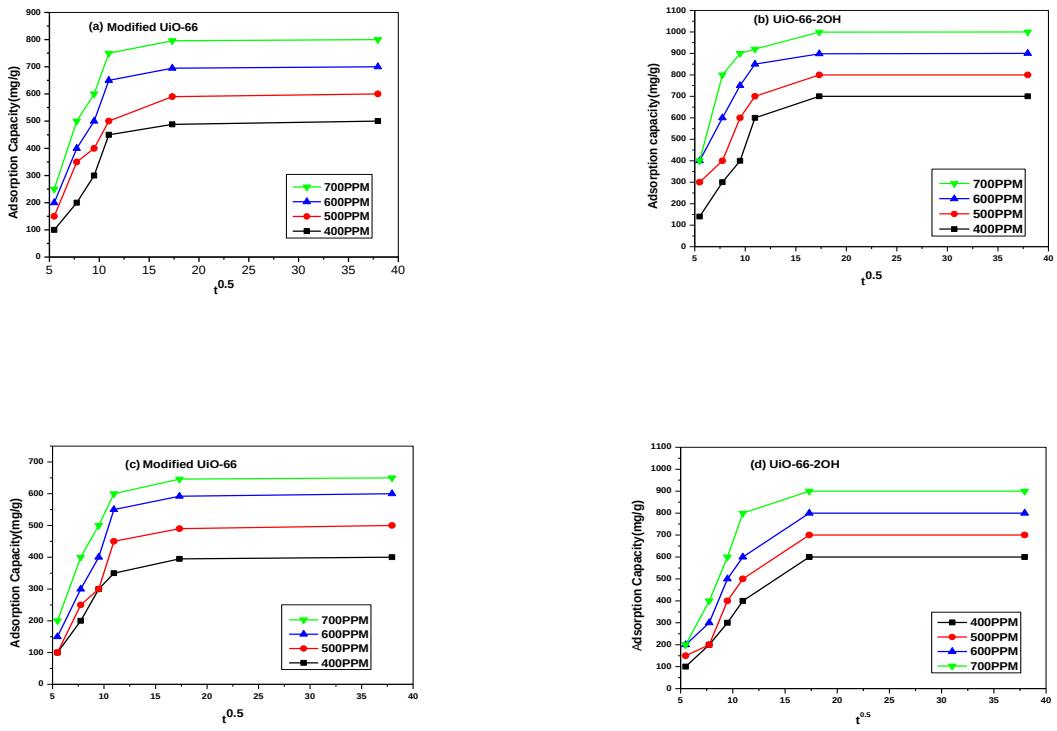

FIG.8 Kinetic adsorption represented by the intraparticle model on modified UiO-66 and UiO-66-2OH at pH = 7 (a, b) and pH = 3 (c, d).

Both modified UiO-66 and UiO-66-2OH demonstrated very high affinity to adsorb MEG molecules in neutral aqueous solutions. Both of them had significant adsorption capacity towards MEG, with modified UiO-66 at 800 mg. g^{-1} and UiO-66-2OH at 1000 mg. g^{-1}. However, the capacities are reduced in acidic conditions (pH = 3) to 650 and 900 mg. g^{-1}, respectively, as shown in Figure 8 (a, b, c, d). Although MEG is a non-electrolyte, this high adsorption of MEG is influenced by several factors. First, a large

pore size in combination with a high pore volume increases the chance of interactions between MEG molecules and the adsorption sites. Nanoscaled particles of modified UiO-66 and UiO-66-2OH may also enhance the adsorption capacity due to the increase in interparticle pores and external surface area with a decrease in particle size [49, 50]. In addition, the highest adsorption was seen on UiO-66-2OH due to its high external surface area and also the presence of hydroxyl groups in MEG molecules, and UiO-66-2OH enriches their interactions via hydrogen bonding which may lead to an increased adsorption capacity. As a matter of fact, the presence of hydroxyl groups enhanced the zeta potential on the surface of UiO-66-2OH. The Zeta potential was -18.43 mV on UiO-66-2OH while it was -5.92 mV on modified UiO-66. Consequently, the electrostatic attraction can be increased, resulting in a high adsorption capacity of UiO-66-2OH. The removal efficiency of MEG from wastewater during contact time of 24 h depends on the initial concentration and the type of adsorbent. From Figure 9, the removal efficiency is at its highest when the initial concentration of MEG is 150 ppm; it was approximately 96% in UiO-66-2OH and 91.6% in modified UiO-66 under the similar conditions (pH = 7, 298 K). Modified UiO-66 also demonstrated lower efficiency than UiO-66-2OH accompanied with variation in the removal rate, as there is a sharp decrease in efficiency when the concentration increases from 300 ppm to 400 ppm [51]. Increasing the initial concentration of MEG may increase the competitive behavior of MEG molecules themselves toward the pore surfaces in modified UiO-66, which does not have attractive functional groups (like hydroxyl groups) as the case of UiO-66-2OH.

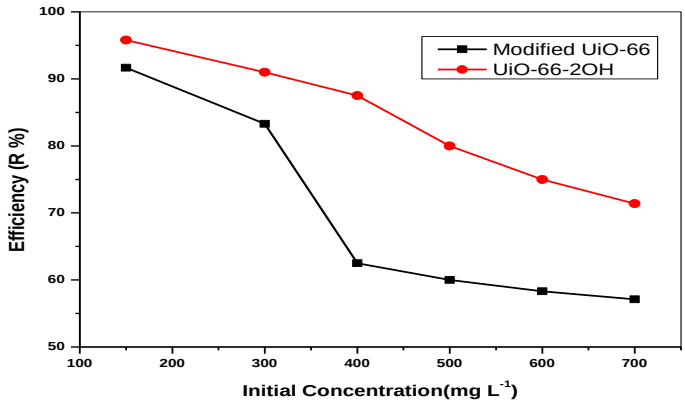

FIG 9 Removal efficiency for MEG solutions of different concentrations in aqueous conditions at pH = 7

Figures S9 and S10 show the removal efficiency of MEG on modified UiO-66 and UiO-66-2OH, respectively, in five cycles. Modified UiO-66 displayed removal efficiency of 42% in the first and second cycles and then stable efficiency at 33.3% in the last three cycles. For UiO-66-2OH, the removal efficiency was 50% in the first three cycles, and then it was dropped to 25% in the fifth cycle. Consequently, the modified UiO-66 and UiO-66-2OH could maintain the removal of MEG from water with relatively strong stability for their practical application.

Sorption Isotherms

It is important to determine the best isotherm that can represent the experimental data. Therefore, two common isotherms were considered when investigating this adsorption isotherm, those being the Langmuir and Freundlich isotherm models. The Langmuir model was derived for the ideal assumption of a uniform homogeneous adsorption surface, while the Freundlich model was designed for application to more heterogeneous surfaces [21].

Langmuir Model

This model assumes a homogeneous surface where all adsorption sites possess identical affinity for solute, and as such contiguous interactions and steric hindrance are non-existent between adsorbed molecules on neighboring sites [52, 53]. The nonlinear form of the Langmuir adsorption isotherm model can be represented as:

$$q_e = \frac{q_m K_l C_e}{1 + K_L C_e} \qquad (4)$$

Equation (4) can be transferred to the following linear form to determine the Langmuir adsorption parameters:

$$\frac{1}{q_e} = \frac{1}{q_m} + \frac{1}{q_m K_l C_e} \qquad (5)$$

where q_e is the amount of MEG adsorbed at equilibrium (mg/g), q_m is a Langmuir constant related to the monolayer coverage capacity (mg/g), K_l is a Langmuir constant

for the adsorption energy, and C_e is the concentration of MEG at equilibrium (mg/L). A linear plot of $1/q_e$ versus $1/C_e$ is used to compute Langmuir isotherm constants in equation (4).

Another equilibrium parameter for the Langmuir isotherm, called the separation factor, may be expressed as R_L (dimensionless) which is related to the adsorption nature [54, 55] as:

$$R_L = \frac{1}{1 + K_L C_o} \quad (6)$$

where C_o is the initial concentration of MEG (mg/L).

Freundlich Model

This model applies primarily to multilayer adsorption on heterogeneous surfaces with different affinities and adsorption heats for the solute. It is normally used to describe non-ideal and reversible adsorption of inorganic and organic components in solution [18, 47], and can be expressed as:

$$q_e = K_f C_e^{\frac{1}{n}} \quad (7)$$

Equation (7) can be rearranged in the following linear form:

$$ln\, q_e = lnK_f + \frac{1}{n} lnC_e \quad (8)$$

where K_f is the Freundlich isotherm constant, which is a rough indicator of adsorption capacity (mg/g), C_e is the equilibrium constant of MEG (mg/g), and n is the adsorption intensity. The magnitude of n may indicate the favorability of an adsorption process, where n >1 indicates favorable normal adsorption while n < 1 denotes cooperative adsorption [54, 56, 57].

Table 3 shows the parameters of the Langmuir and Freundlich models for adsorption of MEG molecules on modified UiO-66 and UiO-66-2OH. Fitting of the experimental data for MEG on modified UIO-66 to the Langmuir isotherm model in Table 3 indicates that q_m is 2.5 times higher than q_e in neutral solution. However, it is 1.4 times as high as the value of q_e in acidic solution. From the correlation parameters (R^2) in Table 3, the experimental data for MEG adsorption on modified UiO-66 at pH = 7 were better fitted to the Langmuir adsorption isotherm model (R^2= 0.99) compared to the

Freundlich isotherm model (R^2=0.90). Therefore, the monolayer coverage is dominant on the external surface area of modified UiO-66 at pH = 7. Conversely, the Freundlich isotherm model had R^2= 0.98 at pH = 3, suggesting multilayer coverage of MEG on modified UIO-66 in acidic aqueous solutions of MEG. This behavior is apparent in Figure 10, and may be attributed to uneven distribution of H^+ on the surface of the adsorbent. On the other hand, adsorption of MEG on UiO-66-2OH was fitted well by the Langmuir isotherm model in neutral and acidic conditions, with R^2 = 0.94 compared to R^2 = 0.92 for the Freundlich model (Table 3 and Figure 11). However, the calculated values of q_m were higher than the corresponding experimental values. The best fit for the adsorption of MEG was observed on modified UiO-66 and UiO-66-2OH using the Langmuir isotherm model in neutral aqueous conditions.

Figures S11 and S12 show the separation factor of the Langmuir constant R_L, which indicates the nature of adsorption onto the adsorbents. Here, 0< R_L <1 denotes favorable normal adsorption over the whole range of initial concentrations used in this study. However, the behavior of MEG molecules differed for adsorption on modified UiO-66 and UiO-66-2OH, based on the acidity of the aqueous MEG solution. R_L for adsorption of MEG on modified UiO-66 is higher in neutral solutions than in acidic solutions, while the highest value is demonstrated by the adsorption of MEG on UiO-66-2OH in acidic conditions. This is caused by the enhanced attractive force for MEG molecules toward the surface of UiO-66-2OH at increasing concentrations of H^+ which are associated with lower pH values.

Table 3 Isotherm parameters for MEG removal on modified UiO-66 and UiO-66-2OH at pH = 3 and 7.

Adsorbent	Langmuir Isotherm			Freundlich Isotherm			
Modified UiO-66	q_m **(mg·g⁻¹)**	K_l **(L·mg⁻¹)**	R^2	$\frac{1}{n}$	n	K_f **(mg·g⁻¹)**	R^2
pH 3	909.1	0.00593	0.94	0.75	1.33	11.4	0.986
pH 7	2000	0.00226	0.99	0.53	1.88	27.8	0.906
UiO-66-2OH							
pH 3	10000	0.0004	0.94	0.92	1.08	6.35	0.902
pH 7	2500	0.0047	0.92	0.56	1.78	47.1	0.836

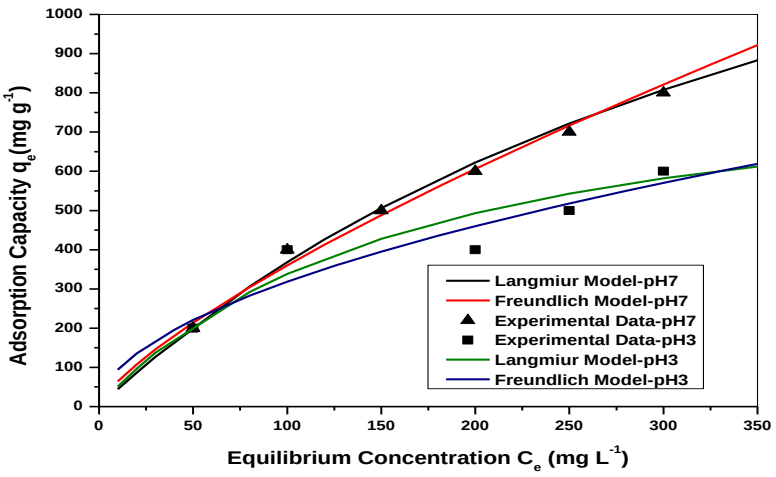

FIG 10 Experimental MEG adsorption isotherms on modified UiO-66 and modelled results using Langmuir and Freundlich models

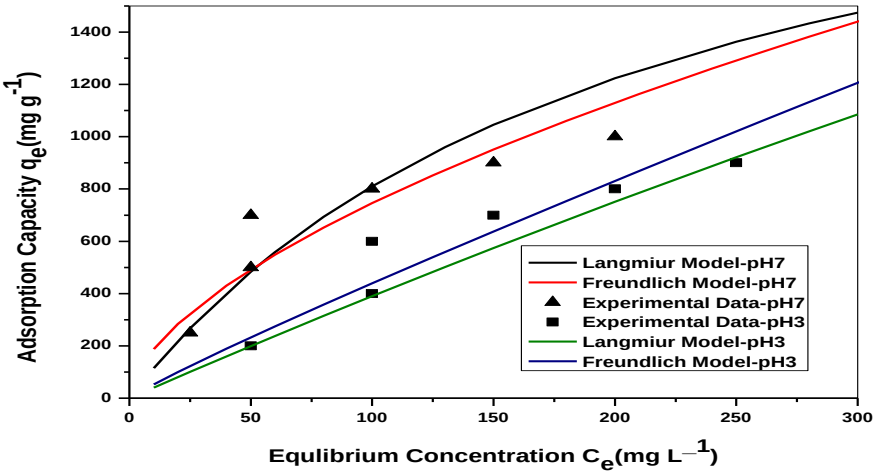

FIG.11 Experimental MEG adsorption isotherms on UiO-66-2OH and fittings using Langmuir and Freundlich models.

Conclusions

MEG exhibits exceptional affinity for adsorption on UiO-66-2OH and modified UiO-66-2OH. The best removal efficiency was achieved on UiO-66-2OH compared to modified UiO-66. The adsorption kinetics were best represented using a pseudo-first order model, while the Langmuir isotherm model suggested monolayer adsorption of MEG on UiO-66-2OH and modified UiO-66. These metal-organic frameworks unprecedentedly removed this pollutant from wastewater and they will make for better adsorbents for the capture of MEG in the effluent wastewater produced in the petroleum industry. Modified UiO-66 exposed higher stability in recycling use than UiO-66-2OH. The results in this study by using MOFs as adsorbents to remove MEG from wastewater have never been seen in previous literatures. It can be recommended that dynamic adsorption by breakthrough experiments should be intensively investigated by using these types of MOFs for MEG removal from wastewater and compared with different metal-based MOFs.

Acknowledgements

We thank Mr. Jason Wright and Mr. Andrew Chan in Chemical Engineering Department and Ms. Elaine Miller in John de laeter Centre at Curtin University for their technical assistance. Also we thank Australian Research Council for partially financial support under project DP170104264.

References

1. Maller, C., et al., *Healthy nature healthy people: 'contact with nature' as an upstream health promotion intervention for populations.* Health Promotion International, 2006. **21**(1): p. 45-54 DOI: 10.1093/heapro/dai032.
2. Orr, D.W., *Earth in mind: On education, environment, and the human prospect*. 2004: Island Press.
3. Da Silva, E.M., et al., *Impact of petroleum pollution on aquatic coastal ecosystems in Brazil.* Environmental Toxicology and Chemistry, 1997. **16**(1): p. 112-118 DOI: 10.1002/etc.5620160112.
4. Harrison, R.M., *An introduction to pollution science*. 2006: Royal Society of Chemistry.
5. Daghetti, A., et al., *Adsorption of aliphatic monoethers of ethylene glycol (alkoxyethanol) at the free water surface and at the Hg/solution interface.* Journal of Electroanalytical Chemistry and Interfacial Electrochemistry, 1986. **204**(1): p. 299-313 DOI: http://dx.doi.org/10.1016/0022-0728(86)80528-9.
6. Esmaeili, A. and K. Loghmani, *Removal of Monoethylene Glycol from Gas Field Wastewater Using Aspergillus tubingensis and a New Bioreactor.* Waste and Biomass Valorization, 2016. **7**(1): p. 151-156.
7. Aguilar-Arteaga, K., J. Rodriguez, and E. Barrado, *Magnetic solids in analytical chemistry: a review.* Analytica Chimica Acta, 2010. **674**(2): p. 157-165.
8. Robinson, M., et al., *Subacute and Subchronic Toxicity of Ethylene Glycol Administered in Drinking Water to Sprague-Dawley Rats.* Drug and Chemical Toxicology, 1990. **13**(1): p. 43-70 DOI: 10.3109/01480549009011069.
9. Aworn, A., P. Thiravetyan, and W. Nakbanpote, *Preparation of CO 2 activated carbon from corncob for monoethylene glycol adsorption.* Colloids and Surfaces A: Physicochemical and Engineering Aspects, 2009. **333**(1): p. 19-25.

10. Devold, H., *Oil and gas production handbook: an introduction to oil and gas production*. 2013: Lulu. com.
11. Orecki, A., et al., *Separation of ethylene glycol from model wastewater by nanofiltration.* Desalination, 2006. **200**(1-3): p. 358-360.
12. Evans, W. and E. David, *Biodegradation of mono-. di-and triethylene glycols in river waters under controlled laboratory conditions.* Water Research, 1974. **8**(2): p. 97-100.
13. Van der Bruggen, B., M. Mänttäri, and M. Nyström, *Drawbacks of applying nanofiltration and how to avoid them: A review.* Separation and Purification Technology, 2008. **63**(2): p. 251-263 DOI: http://dx.doi.org/10.1016/j.seppur.2008.05.010.
14. Teamkao, P. and P. Thiravetyan, *Bioremediation of MEG, DEG, and TEG: Potential of Burhead Plant and Soil Microorganisms.* World Academy of Science, Engineering and Technology, International Journal of Biological, Biomolecular, Agricultural, Food and Biotechnological Engineering, 2012. **6**(10): p. 947-950.
15. Robinson, T., et al., *Remediation of dyes in textile effluent: a critical review on current treatment technologies with a proposed alternative.* Bioresource Technology, 2001. **77**(3): p. 247-255 DOI: http://dx.doi.org/10.1016/S0960-8524(00)00080-8.
16. Mohan, D. and C.U. Pittman, *Arsenic removal from water/wastewater using adsorbents—a critical review.* Journal of hazardous materials, 2007. **142**(1): p. 1-53.
17. Ali, I. and V. Gupta, *Advances in water treatment by adsorption technology.* Nature protocols, 2006. **1**(6): p. 2661.
18. Namasivayam, C. and D. Kavitha, *Removal of Congo Red from water by adsorption onto activated carbon prepared from coir pith, an agricultural solid waste.* Dyes and pigments, 2002. **54**(1): p. 47-58.
19. Monser, L. and N. Adhoum, *Modified activated carbon for the removal of copper, zinc, chromium and cyanide from wastewater.* Separation and purification technology, 2002. **26**(2): p. 137-146.
20. Wang, S. and Y. Peng, *Natural zeolites as effective adsorbents in water and wastewater treatment.* Chemical Engineering Journal, 2010. **156**(1): p. 11-24.

21. Hui, K., C.Y.H. Chao, and S. Kot, *Removal of mixed heavy metal ions in wastewater by zeolite 4A and residual products from recycled coal fly ash.* Journal of Hazardous Materials, 2005. **127**(1): p. 89-101.
22. Lin, K.-Y.A., Y.-T. Liu, and S.-Y. Chen, *Adsorption of fluoride to UiO-66-NH 2 in water: stability, kinetic, isotherm and thermodynamic studies.* Journal of colloid and interface science, 2016. **461**: p. 79-87.
23. Azhar, M.R., et al., *Adsorptive removal of antibiotic sulfonamide by UiO-66 and ZIF-67 for wastewater treatment.* Journal of Colloid and Interface Science, 2017. **500**: p. 88-95.
24. Wang, B., et al., *Highly stable Zr (IV)-based metal–organic frameworks for the detection and removal of antibiotics and organic explosives in water.* J. Am. Chem. Soc, 2016. **138**(19): p. 6204-6216.
25. Li, X., et al., *Mechanistic insight into the interaction and adsorption of Cr (VI) with zeolitic imidazolate framework-67 microcrystals from aqueous solution.* Chemical Engineering Journal, 2015. **274**: p. 238-246.
26. Azhar, M.R., et al., *One-pot synthesis of binary metal organic frameworks (HKUST-1 and UiO-66) for enhanced adsorptive removal of water contaminants.* Journal of colloid and interface science, 2017. **490**: p. 685-694.
27. Lin, K.-Y.A., et al., *Removing oil droplets from water using a copper-based metal organic frameworks.* Chemical Engineering Journal, 2014. **249**: p. 293-301.
28. Khan, N.A., Z. Hasan, and S.H. Jhung, *Adsorptive removal of hazardous materials using metal-organic frameworks (MOFs): a review.* Journal of hazardous materials, 2013. **244**: p. 444-456.
29. Hasan, Z. and S.H. Jhung, *Removal of hazardous organics from water using metal-organic frameworks (MOFs): plausible mechanisms for selective adsorptions.* Journal of hazardous materials, 2015. **283**: p. 329-339.
30. Rada, Z.H., et al., *Functionalized UiO-66 by Single and Binary (OH) 2 and NO2 Groups for Uptake of CO2 and CH4.* Industrial & Engineering Chemistry Research, 2016. **55**(29): p. 7924-7932.
31. Abid, H.R., H.M. Ang, and S. Wang, *Effects of ammonium hydroxide on the structure and gas adsorption of nanosized Zr-MOFs (UiO-66).* Nanoscale, 2012. **4**(10): p. 3089-3094.

32. Abid, H.R., et al., *Nanosize Zr-metal organic framework (UiO-66) for hydrogen and carbon dioxide storage.* Chemical Engineering Journal, 2012. **187**: p. 415-420 DOI: http://dx.doi.org/10.1016/j.cej.2012.01.104.
33. Biswas, S., et al., *Partially fluorinated MIL-47 and Al-MIL-53 frameworks: influence of functionalization on sorption and breathing properties.* Physical Chemistry Chemical Physics, 2013. **15**(10): p. 3552-3561.
34. Haul, R., *Adsorption, Surface Area and Porosity.* Zeitschrift für Physikalische Chemie, 1969. **63**(1_4): p. 220-221.
35. Thommes, M., et al., *Adsorption hysteresis of nitrogen and argon in pore networks and characterization of novel micro-and mesoporous silicas.* Langmuir, 2006. **22**(2): p. 756-764.
36. Furukawa, H., et al., *Water adsorption in porous metal–organic frameworks and related materials.* Journal of the American Chemical Society, 2014. **136**(11): p. 4369-4381.
37. Canivet, J., et al., *Water adsorption in MOFs: fundamentals and applications.* Chemical Society Reviews, 2014. **43**(16): p. 5594-5617.
38. Ghosh, P., Y.J. Colón, and R.Q. Snurr, *Water adsorption in UiO-66: the importance of defects.* Chemical Communications, 2014. **50**(77): p. 11329-11331.
39. Wang, C.-C., et al., *Adsorption of basic dyes onto montmorillonite.* Journal of Colloid and Interface Science, 2004. **273**(1): p. 80-86.
40. Ryu, M.Y., et al., *Effect of the pH and basic additives on the precipitation of calcium carbonate during carbonation reaction.* Resources Processing, 2007. **54**(1): p. 14-18.
41. Abid, H.R., et al., *Adsorption of CH 4 and CO 2 on Zr-metal organic frameworks.* Journal of colloid and interface science, 2012. **366**(1): p. 120-124.
42. Bernal, V., et al., *Effect of Solution pH on the Adsorption of Paracetamol on Chemically Modified Activated Carbons.* Molecules, 2017. **22**(7): p. 1032.
43. Largergren, S., *Zur theorie der sogenannten adsorption geloster stoffe. Kungliga Svenska Vetenskapsakademiens.* Handlingar, 1898. **24**(4): p. 1-39.
44. Ho, Y.-S. and G. McKay, *Pseudo-second order model for sorption processes.* Process biochemistry, 1999. **34**(5): p. 451-465.
45. Graaf, G., et al., *Intra-particle diffusion limitations in low-pressure methanol synthesis.* Chemical Engineering Science, 1990. **45**(4): p. 773-783.

46. de Menezes, E.W., et al., *Ionic silica based hybrid material containing the pyridinium group used as an adsorbent for textile dye.* Journal of colloid and interface science, 2012. **378**(1): p. 10-20.
47. Ho, Y.-S., *Review of second-order models for adsorption systems.* Journal of Hazardous Materials, 2006. **136**(3): p. 681-689 DOI: http://dx.doi.org/10.1016/j.jhazmat.2005.12.043.
48. Dąbrowski, A., et al., *Adsorption of phenolic compounds by activated carbon—a critical review.* Chemosphere, 2005. **58**(8): p. 1049-1070.
49. Kannan, N. and M.M. Sundaram, *Kinetics and mechanism of removal of methylene blue by adsorption on various carbons—a comparative study.* Dyes and pigments, 2001. **51**(1): p. 25-40.
50. Loucks, R.G., et al., *Origin and classification of pores in mudstones from shale-gas systems.* Search and Discovery Article, 2011. **40855**: p. 1-32.
51. Lin, D.-R., et al., *Mechanisms of competitive adsorption organic pollutants on hexylene-bridged polysilsesquioxane.* Materials, 2015. **8**(9): p. 5806-5817.
52. Langmuir, I., *The constitution and fundamental properties of solids and liquids. Part I. Solids.* Journal of the American chemical society, 1916. **38**(11): p. 2221-2295.
53. Chaudhary, N., et al., *Removal of Phenol Using Fly Ash and Impregnated Fly Ash: An Approach to Equilibrium, Kinetic, and Thermodynamic Study.* Separation Science and Technology, 2015. **50**(5): p. 690-699.
54. Dada, A., et al., *Langmuir, Freundlich, Temkin and Dubinin–Radushkevich isotherms studies of equilibrium sorption of Zn2+ unto phosphoric acid modified rice husk.* IOSR Journal of Applied Chemistry, 2012. **3**(1): p. 38-45.
55. Weber, T.W. and R.K. Chakravorti, *Pore and solid diffusion models for fixed-bed adsorbers.* AIChE Journal, 1974. **20**(2): p. 228-238.
56. Mohan, S.V. and J. Karthikeyan, *Removal of lignin and tannin colour from aqueous solution by adsorption onto activated charcoal.* Environmental Pollution, 1997. **97**(1): p. 183-187.
57. Liu, S., *Cooperative adsorption on solid surfaces.* Journal of Colloid and Interface Science, 2015. **450**(Supplement C): p. 224-238 DOI: https://doi.org/10.1016/j.jcis.2015.03.013.

Electronic Supplementary Information (ESI) for

Removal of monoethylene glycol from wastewater by using Zr-metal organic frameworks

Sami Zaboon[a], Hussein Rasool Abid[a],[b*], , Zhengxin Yao[a] , Rolf Gubner[a], Shaobin Wang[a], Ahmed Barifcani[a]

[a] Department of Chemical Engineering, Curtin University, GPO Box U1987, Perth, WA, 6845, Australia.

[b] Environmental Health Department, Faculty of Applied Medical Science, University of Kerbala, Karbala, Iraq

[*]Corresponding author: Tel. +61892665411,

E-mail address: Hussein.Abid@curtin.edu.au, hr_aust2009@yahoo.com.au

Table of Contents

FIG S11 Langmuir isotherm parameter (RL) for adsorption of MEG on modified UiO-66

FIG S12 Langmuir isotherm parameter (RL) for adsorption of MEG on UiO-66-2OH

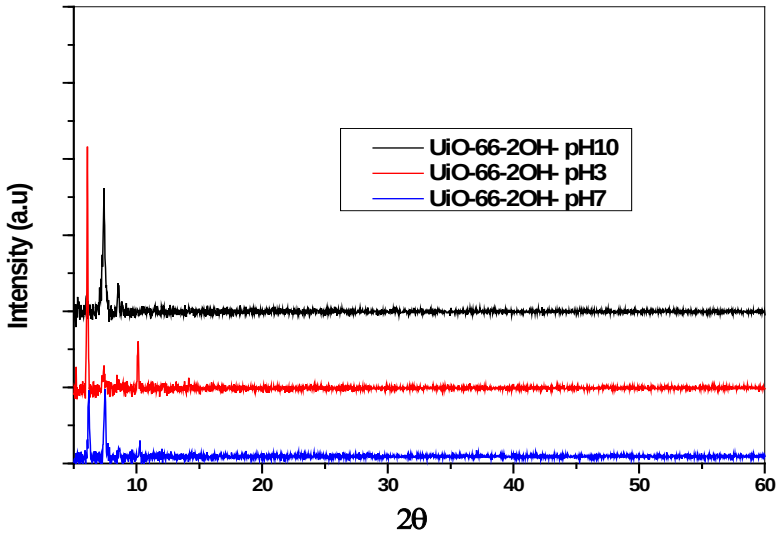

FIG.S1 XRD pattern of UiO-66-2OH in different pH values of MEG solution

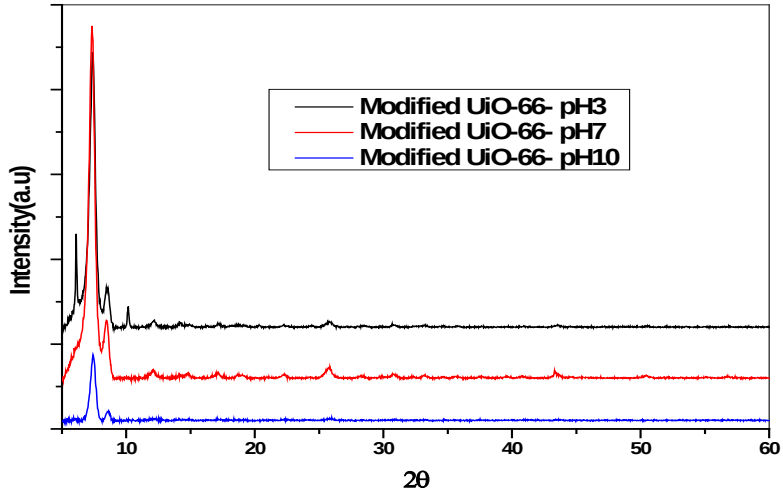

FIG.S2 XRD pattern of modified UiO-66 in different pH values of MEG solution

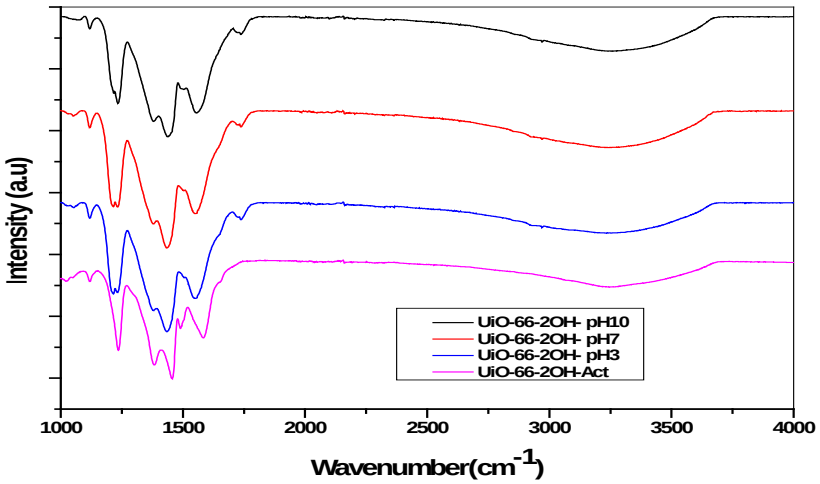

FIG.S3 FTIR spectra of UiO-66-2OH in different pH values of MEG solution

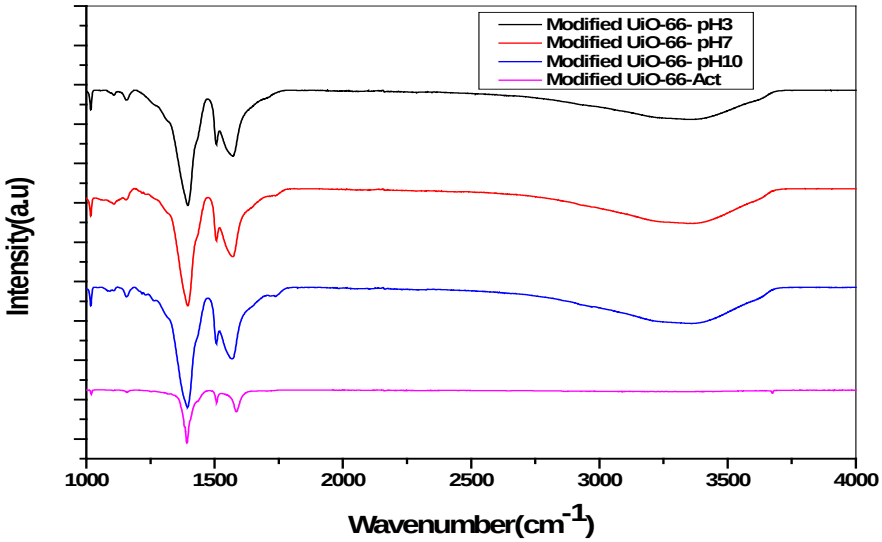

FIG.S4 FTIR spectra of Modified UiO-66 in different pH values of MEG solution

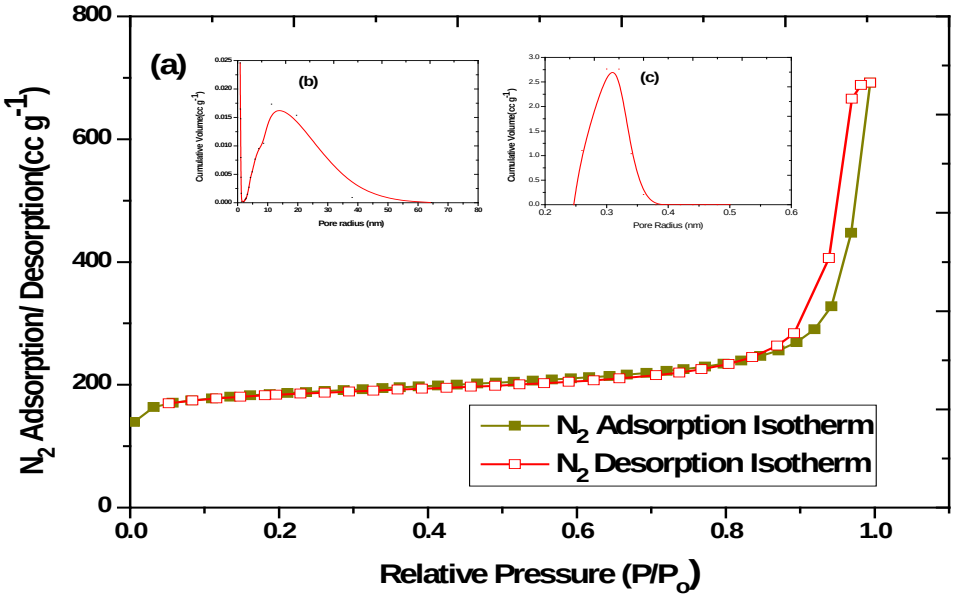

FIG.S5 Adsorption/desorption isotherms of N_2 in modified UiO-66 at 77K, b) Mesopore distribution and c) Micropore distribution after MEG adsorption

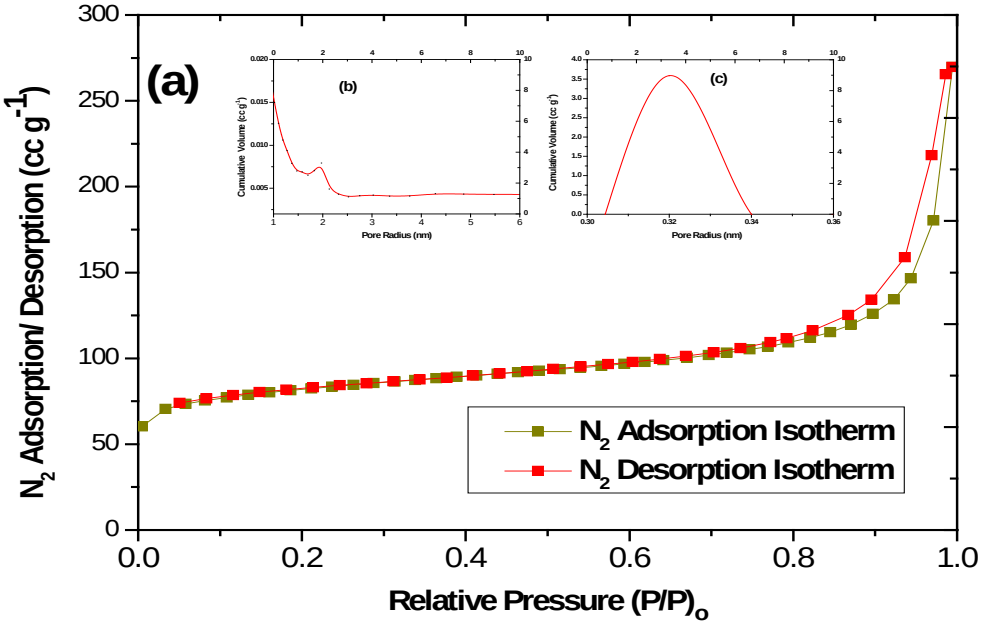

FIG.S6 Adsorption/desorption isotherms of N_2 in UiO-66-2OH at 77K, b) Mesopore distribution and c) Micropore distribution after MEG adsorption

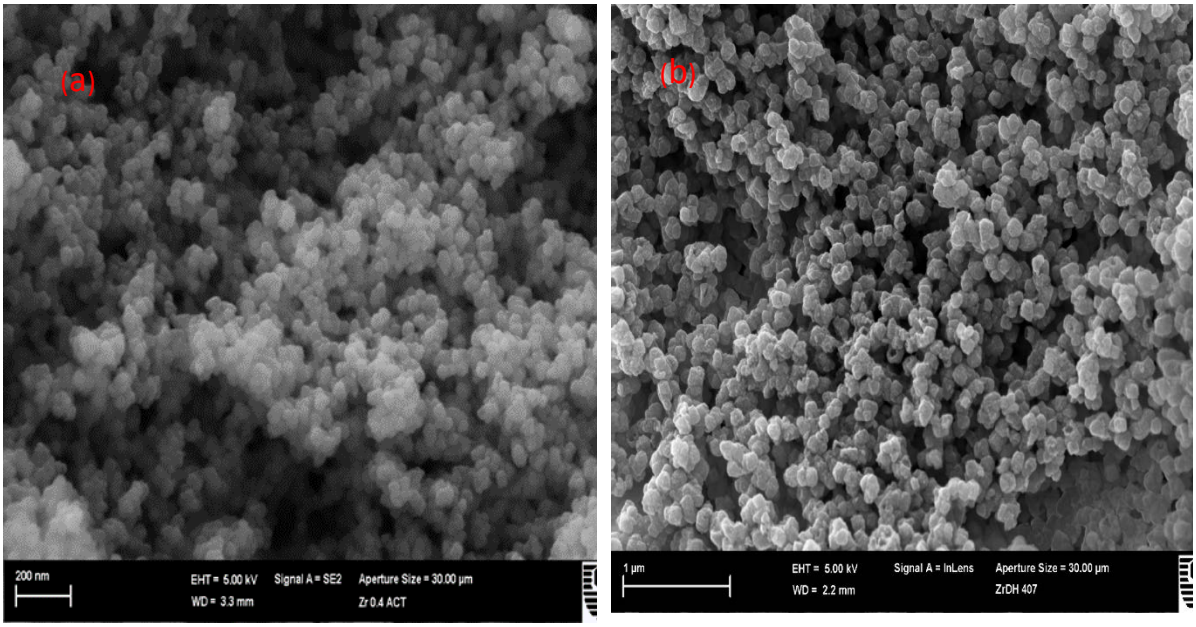

Fig.S7 SEM images of UiO-66-2OH (a) and Modified UiO-66 (b)

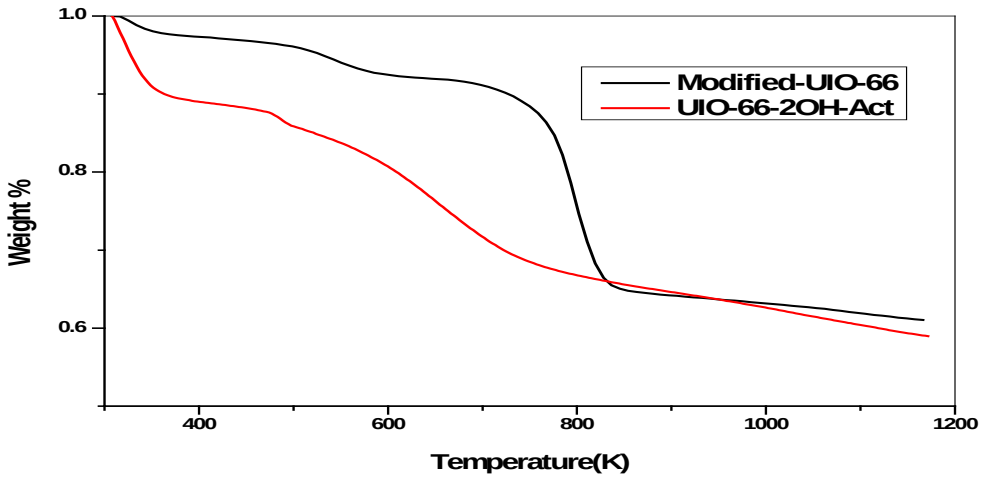

Fig.S8 TGA profiles of Modified UiO-66 and UiO-66-2OH-Act

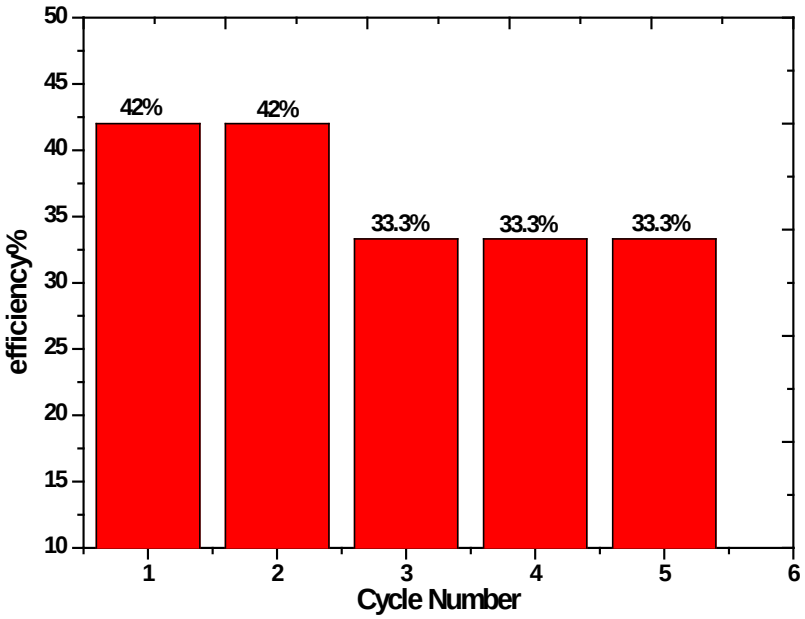

FIG. S9 Removal efficiency of MEG by modified UiO-66 during 60min in different cycles

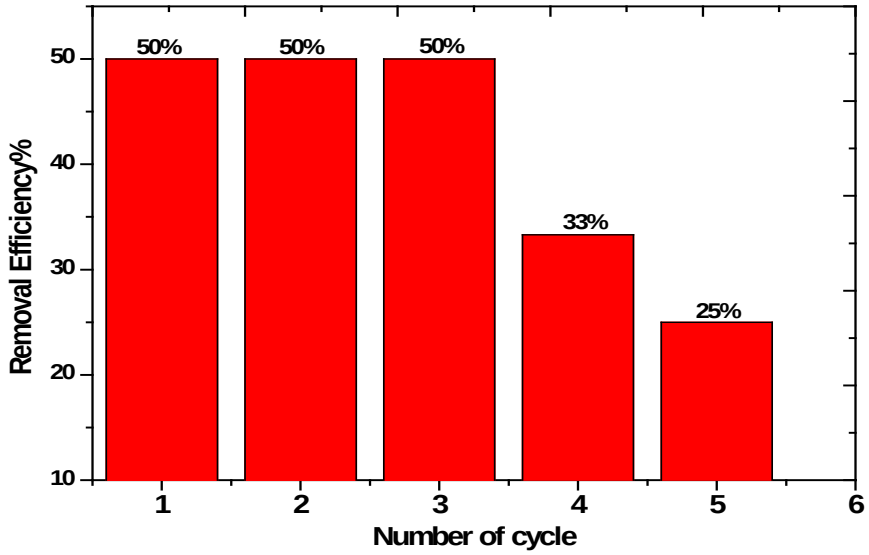

FIG. S10 Removal efficiency of MEG by UiO-66-2OH during 60min in different cycles

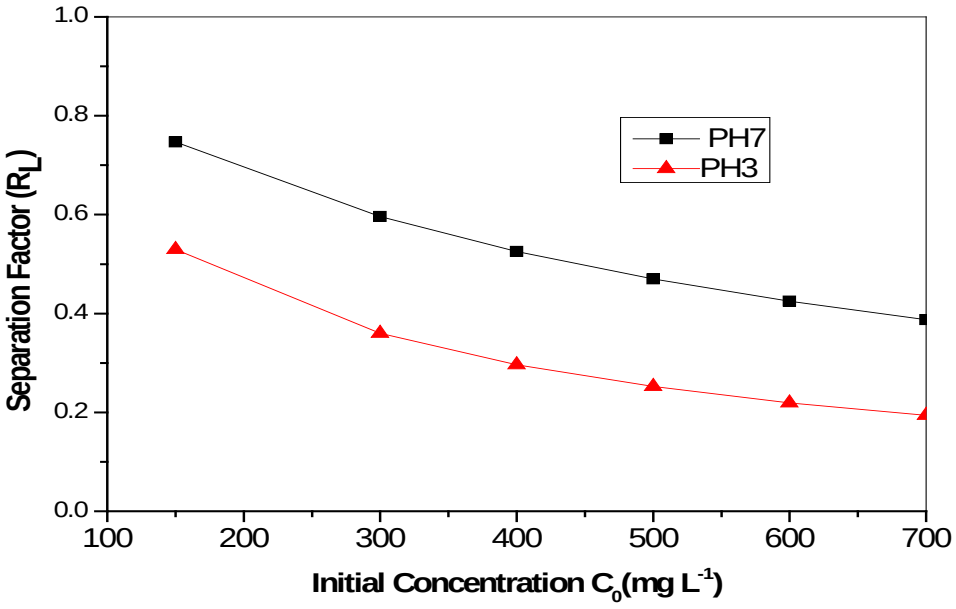

FIG S11 Langmuir isotherm parameter (RL) for adsorption of MEG on modified UiO-66

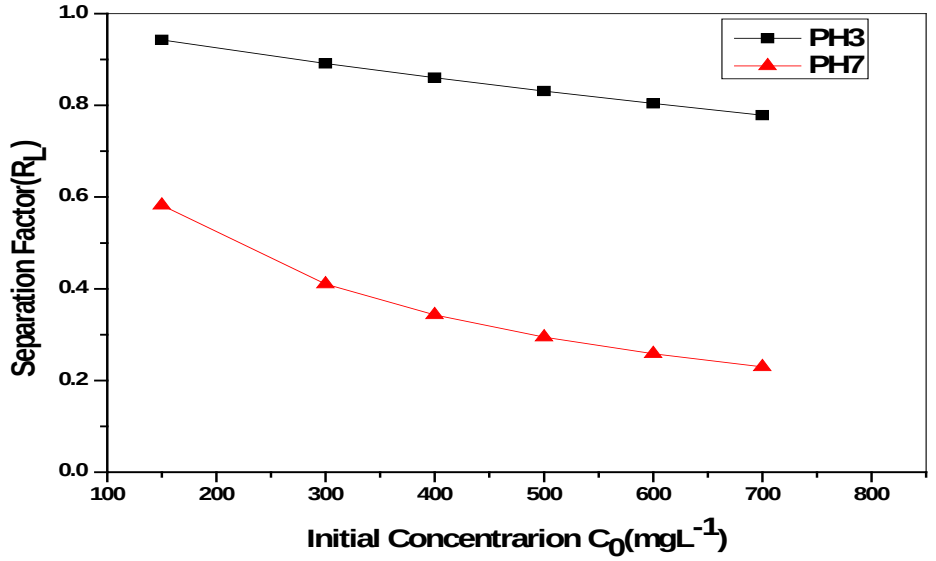

FIG S 12 Langmuir isotherm parameter (RL) for adsorption of MEG on UiO-66-2OH